

# Isoxanthohumol improves obesity and glucose metabolism via inhibiting intestinal lipid absorption with a bloom of *Akkermansia muciniphila* in mice



Yoshiyuki Watanabe<sup>1,10</sup>, Shiho Fujisaka<sup>1,\*,10</sup>, Yoshitomo Morinaga<sup>2</sup>, Shiro Watanabe<sup>3</sup>, Allah Nawaz<sup>1,4</sup>, Hideki Hatta<sup>5</sup>, Tomonobu Kado<sup>1</sup>, Ayumi Nishimura<sup>1</sup>, Muhammad Bilal<sup>1</sup>, Muhammad Rahil Aslam<sup>1</sup>, Keiko Honda<sup>1</sup>, Yoshimi Nakagawa<sup>6</sup>, Samir Softic<sup>7</sup>, Kenichi Hirabayashi<sup>5</sup>, Takashi Nakagawa<sup>8</sup>, Yoshinori Nagai<sup>9</sup>, Kazuyuki Tobe<sup>1,\*\*</sup>

## ABSTRACT

**Objective:** Polyphenols have health-promoting effects, such as improving insulin resistance. Isoxanthohumol (IX), a prenylated flavonoid found in beer hops, has been suggested to reduce obesity and insulin resistance; however, the mechanism remains unknown.

**Methods:** High-fat diet-fed mice were administered IX. We analyzed glucose metabolism, gene expression profiles and histology of liver, epididymal adipose tissue and colon. Lipase activity, fecal lipid profiles and plasma metabolomic analysis were assessed. Fecal 16S rRNA sequencing was obtained and selected bacterial species were used for in vitro studies. Fecal microbiota transplantation and monoclonization were conducted to antibiotic-treated or germ-free (GF) mice.

**Results:** The administration of IX lowered weight gain, decreased steatohepatitis and improved glucose metabolism. Mechanistically, IX inhibited pancreatic lipase activity and lipid absorption by decreasing the expression of the fatty acid transporter CD36 in the small intestine, which was confirmed by increased lipid excretion in feces. IX administration increased markers of intestinal barrier function, including thickening the mucin layer and increasing claudin-1, a tight-junction related protein in the colon. In contrast, the effects of IX were nullified by antibiotics. As revealed using 16S rRNA sequencing, the microbial community structure changed with a significant increase in the abundance of *Akkermansia muciniphila* in the IX-treated group. An anaerobic chamber study showed that IX selectively promoted the growth of *A. muciniphila* while exhibiting antimicrobial activity against some *Bacteroides* and *Clostridium* species. To further explore the direct effect of *A. muciniphila* on lipid and glucose metabolism, we monoclonized either *A. muciniphila* or *Bacteroides thetaiotaomicron* to GF mice. *A. muciniphila* monoclonization decreased CD36 expression in the jejunum and improved glucose metabolism, with decreased levels of multiple classes of fatty acids determined using plasma metabolomic analysis.

**Conclusions:** Our study demonstrated that IX prevents obesity and enhances glucose metabolism by inhibiting dietary fat absorption. This mechanism is linked to suppressing pancreatic lipase activity and shifts in microbial composition, notably an increase in *A. muciniphila*. These highlight new treatment strategies for preventing metabolic syndrome by boosting the gut microbiota with food components.

© 2023 The Author(s). Published by Elsevier GmbH. This is an open access article under the CC BY license (<http://creativecommons.org/licenses/by/4.0/>).

**Keywords** *Akkermansia muciniphila*; Insulin resistance; Isoxanthohumol; Lipid absorption; Microbiota; Obesity

<sup>1</sup>First Department of Internal Medicine, Faculty of Medicine, University of Toyama, Toyama, Japan <sup>2</sup>Department of Microbiology, Faculty of Medicine, University of Toyama, Toyama, Japan <sup>3</sup>Institute of Natural Medicine, University of Toyama, Toyama, Japan <sup>4</sup>Section of Integrative Physiology and Metabolism, Joslin Diabetes Center and Harvard Medical School, Boston, MA, USA <sup>5</sup>Department of Diagnostic Pathology, Faculty of Medicine, University of Toyama, Toyama, Japan <sup>6</sup>Division of Complex Biosystem Research, Department of Research and Development, Institute of Natural Medicine, University of Toyama, Toyama, Japan <sup>7</sup>Department of Pediatrics, Division of Pediatric Gastroenterology, University of Kentucky College of Medicine, Lexington, KY, USA <sup>8</sup>Department of Molecular and Medical Pharmacology, Faculty of Medicine, University of Toyama, Toyama, Japan <sup>9</sup>Department of Pharmaceutical Engineering, Faculty of Engineering, Toyama Prefectural University, Japan

<sup>10</sup> These authors contributed equally.

\*Corresponding author. First Department of Internal Medicine, Faculty of Medicine, University of Toyama, 2630 Sugitani, Toyama, 930-0194, Japan. E-mail: [shihof@med.u-toyama.ac.jp](mailto:shihof@med.u-toyama.ac.jp) (S. Fujisaka).

\*\*Corresponding author. First Department of Internal Medicine, Faculty of Medicine, University of Toyama, 2630 Sugitani, Toyama, 930-0194, Japan. E-mail: [tobe@med.u-toyama.ac.jp](mailto:tobe@med.u-toyama.ac.jp) (K. Tobe).

Received July 7, 2023 • Revision received September 1, 2023 • Accepted September 1, 2023 • Available online 12 September 2023

<https://doi.org/10.1016/j.molmet.2023.101797>

## Abbreviations

8-PN	8-prenylnaringenin
BHI	Brain Heart Infusion
ELSD	evaporative light-scattering detection
eWAT	epididymal white adipose tissue
FMT	Fecal microbiota transplantation
GF	Germ-free
GLP-1	glucagon-like peptide 1
HFD	high-fat diet
IX	Isoxanthohumol
NEFA	non-esterified fatty acid
PCA	Principal component analysis
SCFA	short-chain fatty acid
TG	triglyceride
TGR5	G-protein-coupled bile acid receptor

## 1. INTRODUCTION

The gut microbiota is a core component of metabolic control [1–3]. They outnumber somatic cells in the gut and are active metabolic species, which maintain the homeostasis of biological activities by metabolizing and synthesizing lipids, amino acids, and vitamins, converting bile acids, and maintaining immune function [4]. Moreover, metabolites derived from the gut microbiota, including short-chain fatty acids (SCFA) and secondary bile acids, act as metabolic signaling molecules [5,6]. The gut microbiota is inherently beneficial for energy balance, glucose metabolism, and immune system. However, under dysbiosis state caused by a high-fat diet (HFD) and obesity, the altered microbial structure disrupts metabolic regulation, leading to further obesity and insulin resistance [3]. One of the mechanisms of insulin resistance by dysbiosis is an elevated chronic inflammation derived from metabolic endotoxemia, which is driven by elevated intestinal permeability [7]. Thus, modifying microbial function to restore the energy-regulatory systems and interventions to enhance the intestinal barrier function can improve metabolic dysfunction.

Polyphenols possess antioxidant, antibacterial, and anti-inflammatory properties [8]. They also modify the microbiota to improve glucose metabolism [9,10]. For instance, a natural polyphenol compound, resveratrol, has been shown in various literature to benefit health and improve insulin resistance. One of its mechanisms of action is associated with microbial modification [10]. Polyphenol-rich cranberry extract has been reported to improve obesity, insulin resistance, and liver steatosis in high-fat diet-induced obese mice by increasing the abundance of *Akkermansia muciniphila*, which improves glucose metabolism [11,12]. Thus, dietary components, particularly polyphenols, may be the treatment of choice for metabolic syndrome. Isoxanthohumol (IX), a heat-stable prenylated flavonoid, is synthesized by isomerizing xanthohumol, which is a flavonoid unique to beer hops and is produced in the beer brewing process [13]. Xanthohumol inactivates sterol regulatory element-binding proteins and reduces fatty acid synthesis, thereby regulating lipid metabolism and improving obesity [14]. Additionally, it possesses biological activities that improve glucose metabolism in the presence of the gut microbiota [15]. This corroborates the hypothesis that beer ingredients possess antimicrobial properties [16]. IX has been suggested to improve obesity and insulin resistance in association with changes in the gut microbiota [17,18]. However, the mechanism has not yet been clarified.

Mucin-degrading *A. muciniphila*, a major species of Verrucomicrobia, resides in the mucus layer [19] of humans and rodents. The relative

abundance of *A. muciniphila* decreases obesity and type 2 diabetes [20]. *A. muciniphila* increases the amount of mucus in the intestinal epithelium and enhances the intestinal barrier to improve metabolic endotoxemia, thereby improving insulin resistance and preventing liver damage and atherosclerosis [21]. In addition, oral pasteurized *A. muciniphila* administration improves insulin sensitivity and hyperlipidemia in overweight/obese participants [22], suggesting that *A. muciniphila* is a promising novel therapeutic modality for metabolic dysfunction. However, efficient methods to increase the relative abundance of *A. muciniphila* and the mechanisms underlying host metabolic improvement are poorly understood.

Therefore, we aimed to elucidate the mechanisms of metabolic improvement by IX from the viewpoints of intestinal function and microbial activity.

## 2. METHODS

## 2.1. Animal studies

Male C57BL/6 mice were purchased from Japan SLC Inc. (Tokyo, Japan). The GF C57BL/6 mice were housed in vinyl isolators and obtained by natural mating. The mice were maintained under a 12-h light–dark cycle and provided *ad libitum* access to water and food. Six-week-old mice were divided into groups and fed HFD, HFD + IX, or HFD + IX + antibiotics. The HFD was purchased from Research Diets Inc (NJ, USA). IsoxanthoFlav (IX) was obtained from Hopsteiner (Mainburg, Germany). Each diet was frozen until use and replaced weekly with a fresh diet. Energy intake was calculated by measuring the average weight of food consumed and multiplying it by the number of calories per unit weight of diet. To establish reproducibility, the experiments were conducted in several independent cohorts, and similar trends were observed. For studies involving the measurement of relatively large variations such as body weight, food intake, and glucose tolerance test results, data from several mouse cohorts were verified by considering the cage effect.

In the study using GF mice, the number of mice per group varied because the mice bred in our isolator were used to ensure that the environmental and genetic backgrounds and ages among all the mice were identical. Vinyl isolators were obtained from JIC Corporation (Tokyo, Japan). The feces of GF mice, wood chip bedding, and cotton-wiped isolators were tested for sterility at the Central Institute for Experimental Animals (Kanawaga, Japan) once a month. The animal care policies and experimental procedures were approved by the Animal Experiment Committee of the University of Toyama. We followed the 3R principle of animal experiments, considered cage effects, and used mice divided into at least three cages per group in our experiments.

## 2.2. Culture experiments

Bacteria were cultured at 37 °C in an anaerobic environment (Bactron EZ, Toei Kaisha Ltd., Tokyo, Japan). Brain Heart Infusion (BHI; Becton Dickinson and Company, New Jersey, USA) was used as the culture medium. During co-culturing with IX, BHI and the bacterial solution were cultured at a ratio of 1000:1. The absorbance at 600 nm was measured after 24 h for *Escherichia coli* and after 48 h for other bacteria.

## 2.3. Bacterial transplantation

*A. muciniphila* or *Bacteroides thetaiotaomicron* was cultured with BHI + four supplements (Hemin solution 0.5 mg/mL, Menadion solution 1 mg/mL, L-Cysteine solution 0.1 mg/mL, and resazurin 0.1%) as medium at 37 °C for 48 h in an anaerobic incubator. The culture

medium was centrifuged for 5 min, the supernatant was discarded, the pellet was suspended in 2 mL of PBS, and 200  $\mu$ L was orally administered to mice by gavage.

#### 2.4. Fecal microbiota transplantation

For bacterial transfer into GF mice, fecal microbiota transplantation (FMT) was performed thrice every alternate day by gastric gavage of 200  $\mu$ L filtered feces suspended in saline. Fecal samples were collected from groups of mice that were fed the HFD or HFD + IX diet for 4 weeks. All recipient mice were maintained on a normal diet after the transfer.

#### 2.5. Antibiotics

In the antibiotic cohort, a mixture of vancomycin (0.5 g/L), metronidazole (0.5 g/L), neomycin (0.5 g/L), and ampicillin (0.5 g/L) (Sigma-Aldrich, St. Louis, MO) was administered to mice from 6 weeks of age in drinking water.

#### 2.6. OGTT and ITT

Each OGTT (2 g/kg weight) and intraperitoneal ITT (1.0 unit/kg) was performed after fasting the animals for 4 h. Blood samples were collected from the tail at specific time intervals, and glucose levels were measured using a Stat Strip XP3 (Nipro, Japan). Plasma insulin was measured using the ELISA kit (Shibayagi, Japan).

#### 2.7. Bomb calorimetry

Feces were collected from each mouse for 24 h. After drying at 50  $^{\circ}$ C for 16 h, the energy contents in the feces were measured with an IKA calorimeter C6000 (IKA, Osaka, Japan) according to the manufacturer's instructions.

#### 2.8. Triglyceride and non-esterified fatty acid analyses

The feces excreted over 24 h were collected and air-dried. After the feces were weighed and pulverized with a mortar and pestle, 100 mg-portion of the fecal powder were used for the extraction of total lipids according to the method of Bligh and Dyer. The fecal total lipids were applied to preparative silica gel thin-layer chromatography (TLC) plates and NEFAs and TGs were isolated by developing the plates with the mixture of petroleum ether, diethyl ether and acetic acid (80:30:1, v/v/v). Fatty acid methyl esters (FAMES) were prepared from the NEFAs and TGs fractions, which were analyzed by gas-liquid chromatography as described previously [23].

#### 2.9. Analysis of TG levels in the liver and plasma

The liver and plasma TG levels were measured using a Triglyceride Colorimetric Assay Kit (Cayman Chemical Company, U.S.A.), according to the manufacturer's instructions.

#### 2.10. Fecal mucin measurement

Fecal mucin levels were determined based on the fluorometric measurement of O-linked reducing sugars using a commercially available kit (Cosmo Bio, Tokyo, Japan). Images were obtained using a microscope connected to a digital camera (BZ-X800; Keyence, Osaka, Japan).

#### 2.11. Pancreatic lipase activity

Pancreatic lipase activity was measured based on the amount of NEFAs generated during the incubation with olive oil emulsified with 5% Gum Arabic solution and porcine pancreatic lipase. IX was dissolved at the desired concentrations in DMSO, which was added to the reaction mixture 5 min before adding porcine pancreatic lipase. The

effects of the test compounds on pancreatic lipase activity were expressed as percentages of the control values which were obtained from the incubation of the reaction mixture containing only DMSO.

#### 2.12. RNA isolation and RT-PCR

Total RNA was extracted from tissues using the RNeasy kit (Qiagen, Hilden, Germany) and reverse transcribed using the TaKaRa Prime-Script RNA Kit (cat# RR036A, Takara, Japan), according to the manufacturer's instructions. Quantitative PCR was performed using the TaqMan method (1 cycle at 50  $^{\circ}$ C for 2 min, 95  $^{\circ}$ C for 10 min, 40 cycles at 95  $^{\circ}$ C for 15 s, and 60  $^{\circ}$ C for 1 min) or the SYBR Green method (1 cycle at 95  $^{\circ}$ C for 30 s, 45 cycles at 95  $^{\circ}$ C for 10 s, and 60  $^{\circ}$ C for 20 s). Each sample was run in duplicate, and the relative mRNA levels were calculated using a standard curve and normalized to the mRNA levels of  $\beta$ -actin or GAPDH. The primer sequences used are listed in the Supplementary Table.

#### 2.13. 16S rRNA sequencing analysis

DNA was extracted from mouse cecal contents or feces using the QIAmp PowerFecal DNA kit (QIAGEN, CA, USA). A multiplexed amplicon library converting the 16S rDNA V4 region was generated from the DNA samples, and sequencing was performed in the Bioengineering Lab. Co., Ltd. (Kanagawa, Japan). Principal component analysis (PCA) was performed using the `prcomp` command in R version 3.2.1. The database consisted of Greengene's 97 operational taxonomic units attached to the microbiota analysis pipeline, Qiime.

#### 2.14. Histological and immunohistochemical analysis

Sections of the liver, epididymal white adipose tissue (eWAT), and colon were excised and immediately fixed in 4% formaldehyde at room temperature. Paraffin-embedded tissue sections were cut into 4  $\mu$ m slices and placed on slides. Sections were stained with H&E or Alcian blue, according to standard procedures. Anti-CD36 antibody was purchased from Abcam (Cambridge, CB2 0AX, UK).

#### 2.15. Metabolome analysis (Dual Scan)

Metabolome analysis was conducted according to the HMT Dual Scan package using capillary electrophoresis time-of-flight MS and liquid chromatography time-of-flight MS in Human Metabolome Technologies Inc. (Japan).

#### 2.16. Western blotting

Proteins were extracted using 1  $\times$  radioimmunoprecipitation assay buffer containing 0.1% sodium dodecyl sulphate. Protein samples (18  $\mu$ g) were subjected to SDS-PAGE and transferred to polyvinylidene fluoride membranes. Primary antibodies for  $\beta$ -actin (1:3000) were purchased from Cell Signaling Technology (Danvers, MA), claudin-1 was purchased from Invitrogen (1:200), and CD36 was from Abcam (1:100). Horseradish peroxidase-conjugated secondary antibodies were purchased from GE Healthcare (Japan) (1:1000). The intensities of the bands were detected using a ChemiDoc Touch MP system (Bio-Rad). ImageJ software was used for quantification.

#### 2.17. Isolation of intestinal cells

Intestinal cells, including intestinal epithelial cells (IECs), were isolated as previously described (Cell Mol Gastroenterol Hepatol 2020; 10:209–223) with slight modifications.

#### 2.18. Statistical analyses

Statistical analyses were performed using the GraphPad Prism 9 software (version 9.4.1; GraphPad Software, San Diego, CA, USA). The

Shapiro-Wilk test was used to check the Gaussian distribution. Data are expressed as the means  $\pm$  standard error of mean. \* $P < 0.05$ , \*\* $P < 0.01$ , \*\*\* $P < 0.001$ , and \*\*\*\* $P < 0.0001$  were considered significant as determined using the unpaired two-tailed  $t$  test, Wilcoxon rank sum test, Mann-Whitney U-test, the Benjamini-Hochberg post-test or analysis of variance (ANOVA) followed by Bonferroni's multiple comparison test or Tukey-Kramer post hoc. Each dot represents a biological sample.

### 3. RESULTS

#### 3.1. IX suppresses body weight gain and improves glucose metabolism in mice on an HFD

HFD-fed C57BL/6 mice were fed a HFD supplemented with IX at 0.1%, according to the previous study [18]. IX significantly decreased body weight (Figure 1A) without altering approximate food intake (Figure 1B). OGTT and ITT confirmed improved glucose metabolism (Figure 1C–E), which was associated with decreased liver weight and improved steatosis (Figure 1F and G). Increased cecum size was observed in the HFD + IX group, suggesting an altered intestinal environment after the intervention (Figure 1F). Consistent with the altered liver weight, IX administration significantly reduced hepatic and plasma TG levels (Figure 1H and I). Crown-like structures in the eWAT clearly decreased (Figure 1J). The expressions of M1 macrophage related genes such as *F4/80*, *Cd11c*, and *Tnfa* was downregulated, and metabolically favorable markers such as *Pgc1-a*, *Pgc1-b*, *Pparg*, and *adiponectin* were upregulated in the eWAT of IX group (Figure 1K). Next, we examined the effect of IX on thermogenesis-related genes such as *Ucp-1*, *Pgc1-a*, and *Cidea* in the inguinal adipose tissues which were unaffected by IX treatment (Suppl Fig. 1). Thus, IX administration improved glucose metabolism and decreased body weight gain in HFD-fed mice.

#### 3.2. IX pharmacologically inhibits lipid absorption

To further elucidate the mechanism of anti-obesity effect of IX administration, the amount of energy in the feces was analyzed with a bomb calorimeter. IX increased energy contents in the feces (Figure 2A). Furthermore, we estimated the fecal lipid excretion by determining the lipid contents. The amounts of many types of fatty acids found in the NEFA and TG fractions from the fecal lipids were significantly increased by IX, suggesting that IX inhibited lipid absorption (Figure 2B and C).

IX is known to be converted to 8-prenylnaringenin (8-PN) via hepatic cytochrome P450-mediated demethylation or can be metabolized by gut bacteria (Figure 2D) [24]. To explore the mechanism underlying the inhibition of fatty acid absorption by IX, we assessed the lipid digestive capacity and found that, both, IX and 8-PN inactivated pancreatic lipase activity by approximately 50–60% (Figure 2E). On the other hand, the expression of *Cd36*, a major lipid transporter was significantly downregulated in line with decreased lipoprotein lipase, *Ppara*, and *Erra* expressions in the small intestine of mice treated with HFD + IX (Figure 2F). These data indicate that IX or its metabolite 8-PN inhibit the breakdown of dietary TGs and lower absorption of fatty acids from the small intestine.

Further, we tested whether IX or 8-PN directly regulates fatty acid transporter gene expression in cultured intestinal epithelial cells (IECs) (Supplementary Fig. 2A). The expression of *Cd36*, *Fabp1*, and *Fatp4* was not altered by the treating isolated intestinal cells, including IECs, with IX or 8-PN for 24 h (Supplementary Fig. 2B). Thus, IX and 8-PN did not directly regulate the expression of fatty acid transporter-related genes in these cells.

We also performed a plasma metabolomic analysis to identify the metabolites altered by IX administration. Heatmap and PCA did not reveal significant differences (Supplementary Figs. 3A and B). Volcano plots showed that the IX treatment significantly altered a small set of seven metabolites (Supplementary Fig. 3C), including oleanolic acid and homoarginine. As these metabolites have been suggested to improve insulin resistance in previous studies, these changes may improve glucose metabolism by IX [25–27]. The two other metabolites were phytosterols such as sitosterol and campesterol (Supplementary Fig. 3C). To determine the metabolic effects of these two phytosterols that were decreased by IX treatment, the mice were treated with phytosterol for 11 weeks. This had no effect on the body weight of mice fed either chow diet or HFD (Supplementary Fig. 3E). On chow diet, phytosterol administration increased fasting blood glucose, but did not affect glucose tolerance on chow or HFD (Supplementary Fig. 3F). Thus, the reduction of plasma phytosterols by IX administration had less effect on obesity or glucose metabolism.

#### 3.3. The favorable metabolic effects of IX treatment are nullified by the elimination of gut microbiota

Cecal weight significantly increased in IX-treated mice (Figure 1E). Since the cecum size can reflect altered gut microbiota [25], we evaluated the metabolic effects of IX treatment without the influence of the microbiota. Interestingly, eliminating gut microbiota by antibiotic treatment nullified the IX-induced metabolic improvements, such as body weight, glucose metabolism, and tissue weight (Figure 3A–D). Antibiotic treatment resulted in an even greater cecal weight, reflecting a marked decrease in microbial content in the intestine (Figure 3D), in agreement to what is known for GF mice [25]. Fecal TG content was elevated in the IX group, which significantly decreased after antibiotic treatment (Figure 3E). These results highlight the favorable metabolic effects of IX treatment only in the presence of intact gut microbiota. To determine the effects of the microbiota established by IX treatment, 8-week-old GF mice were colonized with the microbiota from either HFD- or HFD + IX-fed mice for 5 weeks (Supplementary Fig. 4A). The cecum of the recipient mice given HFD + IX was enlarged, reflecting the donor phenotype, suggesting the viability of the transplanted bacteria (Supplementary Fig. 4B). Although the effect of FMT from HFD + IX donors on liver weight was not altered at 13 weeks age (Supplementary Fig. 4B), body weight and glucose tolerance tended to improve transiently (Supplementary Fig. 4C and D). These metabolic changes were relatively minor, probably because the animals were fed a chow diet.

#### 3.4. IX impacts the microbial community structure and promotes the growth of *A. muciniphila*

Rarefaction curves obtained from 16S rRNA sequencing analysis of fecal samples revealed IX-induced reduction in species richness and evenness (Figure 4A), suggesting the predominance of certain bacterial species. Principal coordinate analysis of weighted UniFrac distances showed a clear separation in the microbial community structures before and after the HFD or HFD + IX challenge (Figure 4B). IX increased the relative abundance of the phylum Verrucomicrobia and decreased those of Firmicutes and Deferribacteres (Figure 4C). At the lower phylogenetic tree level, various bacteria, such as *Mucispirillum*, *Lactobacillus*, Clostridiales, and Clostridiaceae, were eliminated after IX treatment (Figure 4D). In contrast, some bacteria classified as *Parabacteroides*, *Sutterella*, *Enterobacteriaceae*, and *A. muciniphila* were elevated in the IX group (Figure 4D). Since *A. muciniphila* has beneficial effects on glucose metabolism and was most significantly increased by IX treatment, we followed the time course of the

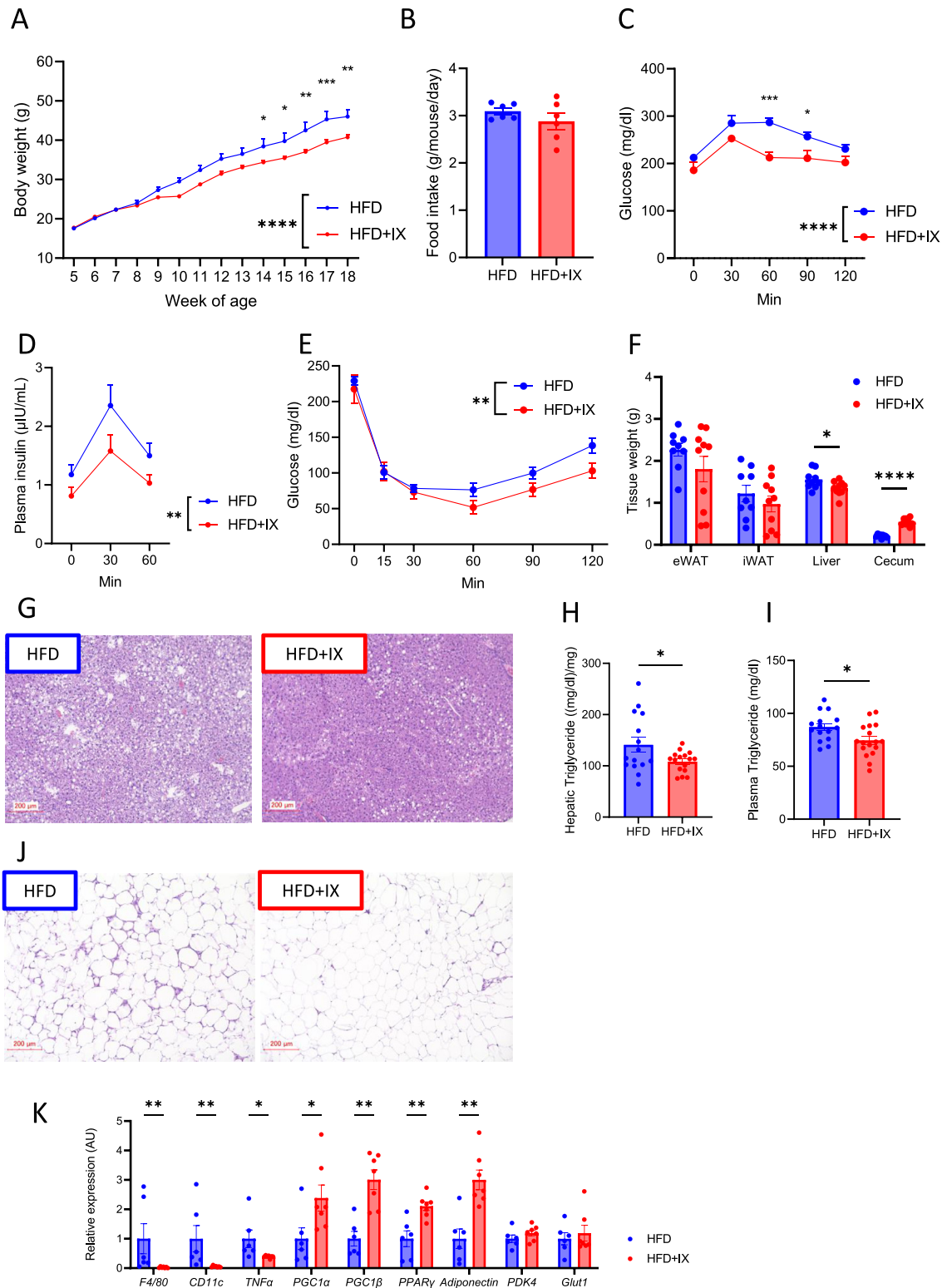


**Figure 1:** Isoxanthohumol (IX) suppresses body weight gain and improves glucose metabolism in mice on a high-fat diet (HFD). (A) Body weight and (B) daily food intake of mice treated with either an HFD (blue) or an HFD + IX (red) ( $n = 9-10$  per group). (C) Oral glucose tolerance test (OGTT), (D) plasma insulin levels at 17 weeks old and (E) insulin tolerance test (ITT) at 16 weeks old. (F) Tissue weight at 20 weeks old ( $n = 9-10$  per group). (G, J) Representative hematoxylin and eosin (H&E)-stained pictures of (G) liver and (J) epididymal adipose tissue at 20 weeks old. Scale bars, 200  $\mu\text{m}$ . (H) Hepatic and (I) plasma triglyceride concentrations at 20 weeks old ( $n = 15-17$  per group). (K) Quantitative PCR analysis of inflammatory and metabolic markers in the epididymal adipose tissues at 20 weeks old ( $n = 6-7$  per group). \* $P < 0.05$ , \*\* $P < 0.01$ , \*\*\* $P < 0.001$ , \*\*\*\* $P < 0.0001$ , by two-way analysis of variance (ANOVA) followed by Bonferroni's multiple comparison tests (A, C, D, E) or unpaired two-tailed  $t$  test (B, F, H, I). \* $P < 0.05$ , \*\* $P < 0.01$ , \*\*\* $P < 0.001$ , followed by the Benjamini-Hochberg post-test ( $q < 0.05$ ) (K). Data are presented as the mean  $\pm$  SEM.

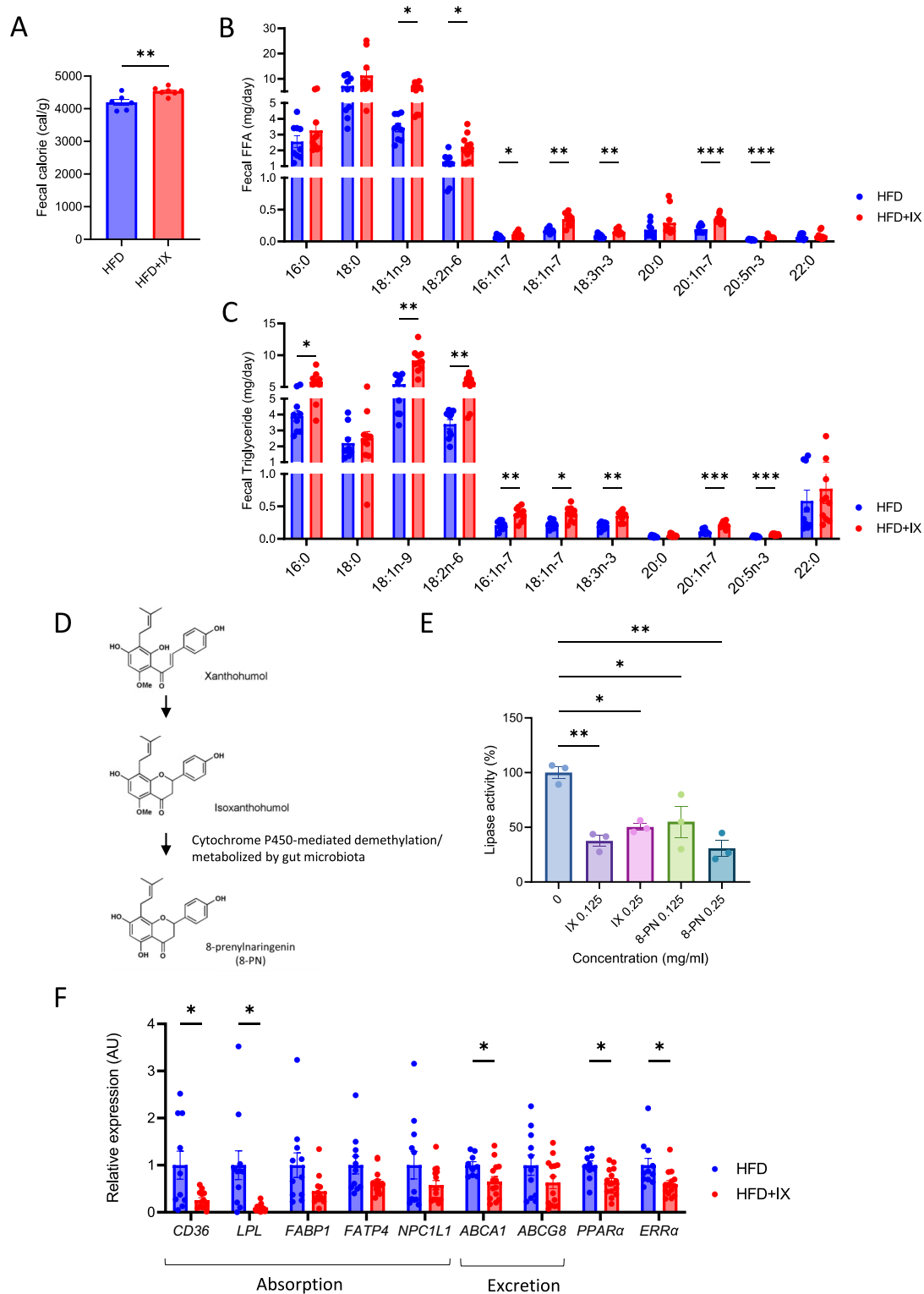


**Figure 2:** IX promotes intestinal lipid excretion. (A) Amount of energy in feces collected for 24 h from each mouse ( $n = 6-7$  per group). (B, C) Concentrations of various classes of (B) fatty acids and (C) triglycerides in feces collected at 24 h from each mouse ( $n = 9-10$  per group). (D) A simplified metabolic pathway of xanthohumol in the gut microbiota. (E) Lipase activity of IX and 8-prenylaringenin at the indicated concentrations ( $n = 3$  per group). (F) qPCR analysis of various lipid transporter-related genes in the jejunum of mice at 18 weeks old ( $n = 11-14$  per group). \* $P < 0.05$ , \*\* $P < 0.01$ , \*\*\* $P < 0.001$ , by unpaired two-tailed  $t$  test for (A), unpaired  $t$ -test or Mann-Whitney U-test followed by the Benjamini-Hochberg post-test ( $q < 0.05$ ) (F) and ANOVA, followed by Tukey-Kramer post hoc for (E). \*adjusted  $P < 0.05$ , \*\*adjusted  $P < 0.01$ , \*\*\*adjusted  $P < 0.001$ , by multiple Mann-Whitney U tests (B and C). Data are presented as the mean  $\pm$  SEM.

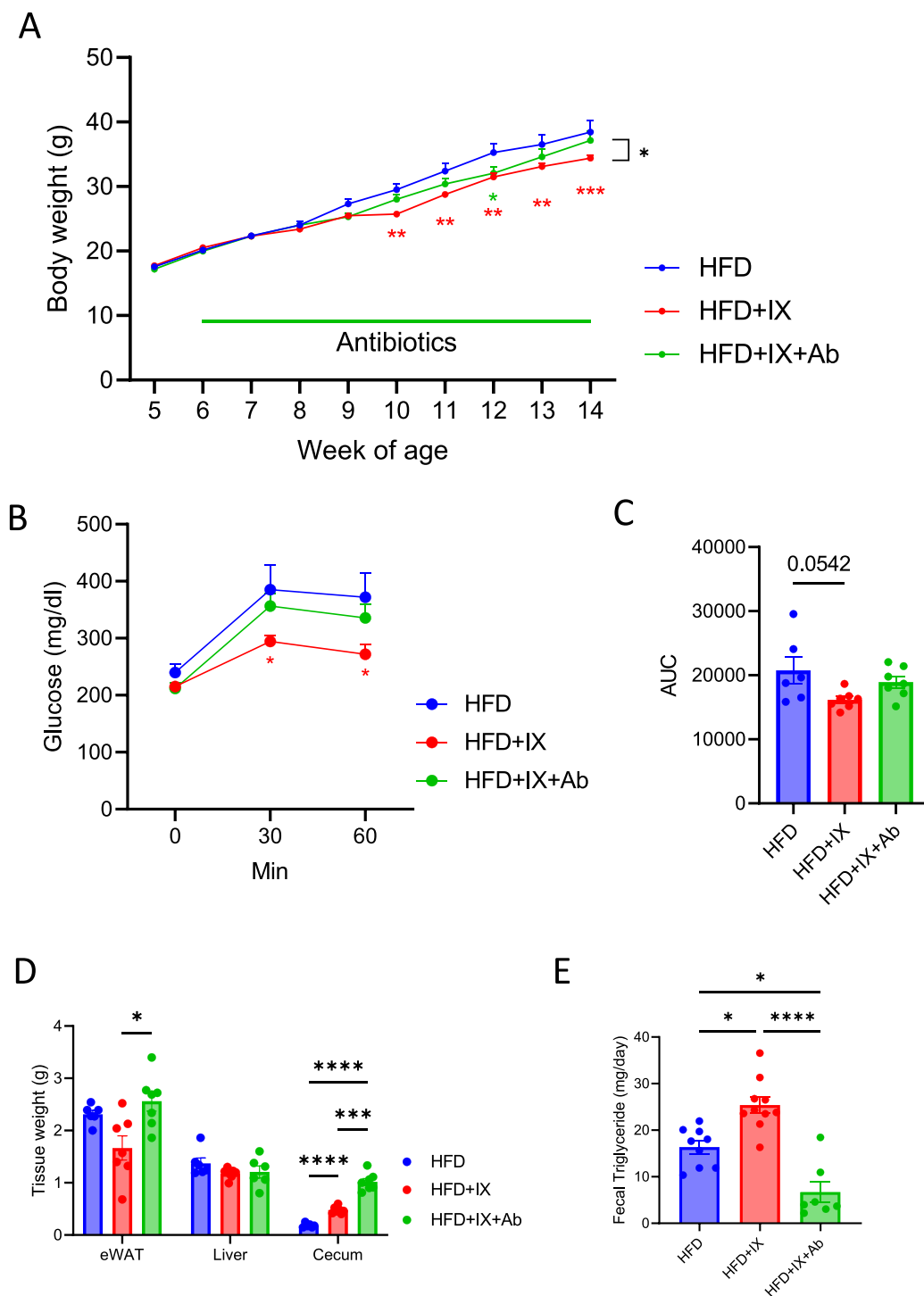


**Figure 3:** The gut microbiota established by IX improves metabolic dysfunction. (A) Body weight of mice treated with either an HFD (blue), an HFD + IX (red) or an HFD + IX + antibiotics (green) ( $n = 6-7$  per group). (B) OGTT at 15 weeks old and (C) area under the curve (AUC) measured during OGTT ( $n = 6-7$  per group). (D) Tissue weight at 18 weeks old ( $n = 6-7$  per group). (E) Fecal triglyceride concentrations ( $n = 7-10$  per group). \* $P < 0.05$ , \*\* $P < 0.01$ , \*\*\* $P < 0.001$ , \*\*\*\* $P < 0.0001$ , using ANOVA, followed by Tukey-Kramer postdoc for (A, C, D, E). Data are presented as the mean  $\pm$  SEM.

quantitative changes after the intervention. While eubacterial DNA levels, which reflect the total bacterial biomass, were not altered by IX treatment for at least the first 4 weeks, the relative abundance of *A. muciniphila* markedly increased after 1 week (Figure 4E and F).

To investigate mechanisms for the proliferation of *A. muciniphila*, we evaluated the effects of IX on bacterial proliferation using an anaerobic chamber. The in vitro study showed that IX selectively promoted the growth of *A. muciniphila* in pure cultures, but not that of other bacteria

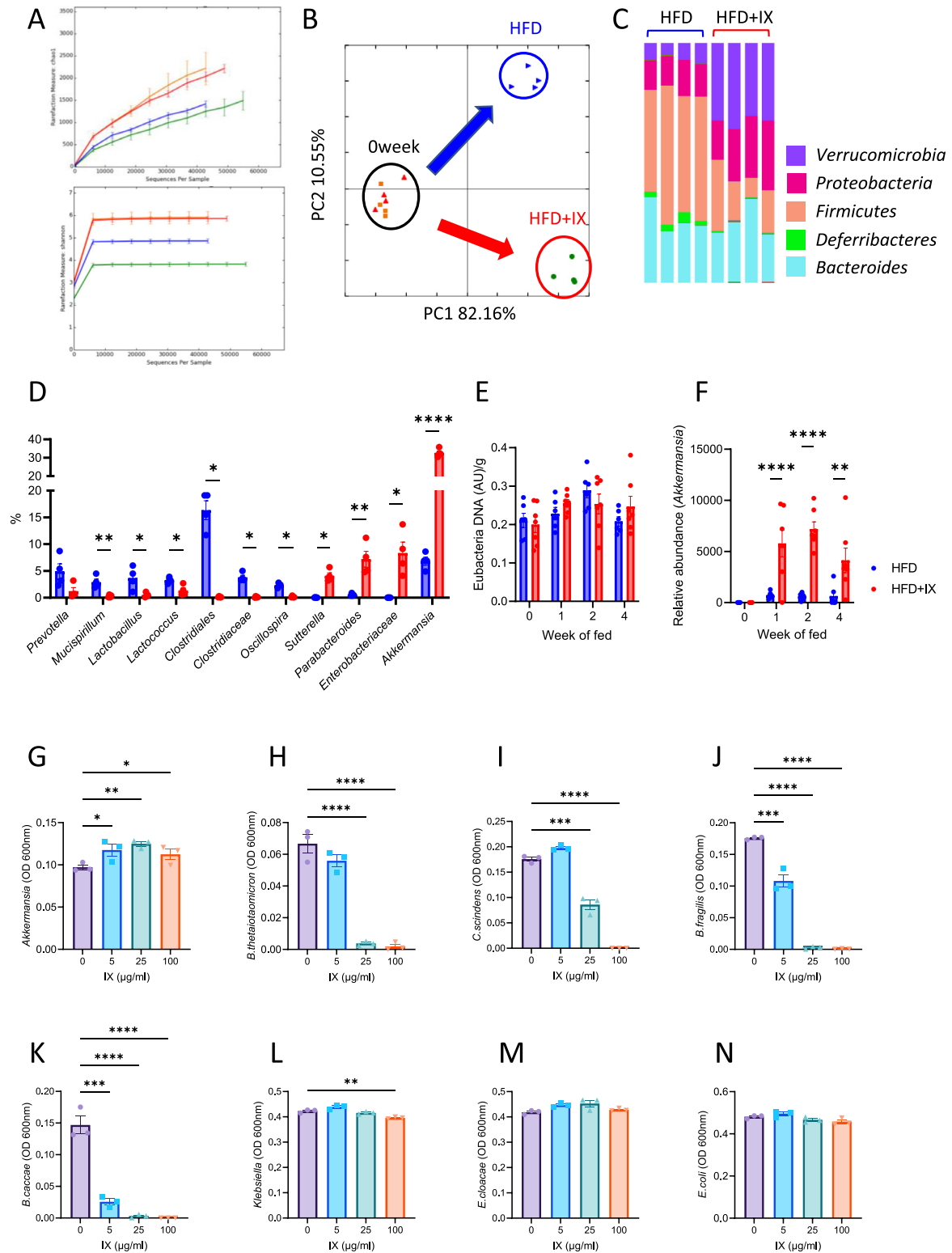


**Figure 4:** IX promotes the growth of *A. muciniphila*. (A) Rarefaction curves of Chao1 and Shannon entropy of fecal 16S rRNA sequencing data from HFD-fed mice with or without IX for 2 weeks (red: pre-HFD, blue: post-HFD orange: pre-HFD + IX, green: post-HFD + IX). (B) Principal coordinate analysis of weighted UniFrac distances. (C) Representation of bacterial phyla in the fecal bacteria of HFD-fed mice with or without IX for 2 weeks. (D) Relative abundances of bacteria that showed significant differences between the HFD and HFD + IX groups (n = 4 per group). (E) Eubacterial DNA levels per gram of feces at different time points (n = 6–7 per group). (F) Relative abundance of *A. muciniphila* normalized to eubacterial levels (n = 6–7 per group). (G)–(N) Growth of bacteria as single cultures in the presence or absence of IX at the indicated concentrations. \*P < 0.05, \*\*P < 0.01, \*\*\*P < 0.001, \*\*\*\*P < 0.0001, by unpaired *t*-test or Wilcoxon rank sum test (D, E) and ANOVA, followed by Bonferroni’s multiple comparison test (F) or Tukey-Kramer post dot for (G–N). Data are presented as the mean ± SEM.



examined (Figure 4G–N). Thus, IX significantly altered the microbial community structure, likely by promoting the growth of *A. muciniphila* and inhibiting the growth of other bacteria, thereby relatively increasing *A. muciniphila* in the intestine.

### 3.5. IX increased mucin levels in the feces and claudin 1 in the colon

Interventions to increase the abundance of *A. muciniphila* have been reported to improve intestinal barrier function [21]. Hence, we further examined whether the intestinal environment with IX-induced proliferation of *A. muciniphila* affects gut barrier-related factors. IX administration thickened the mucus layer of the colon (Figure 5A), which was confirmed by quantification of the fecal mucin levels (Figure 5B). Although intestinal barrier function-related genes were not altered by IX administration (Supplementary Fig. 5), tight junction-related claudin 1 protein levels increased significantly in the IX group (Figure 5C–D). This was associated with the decreased expression of lipopolysaccharide-binding protein (LBP), an endotoxin marker, in the liver (Figure 5E), although the difference was not significant. Thus, IX improved markers of colonic barrier function and likely promoted proliferation of *A. muciniphila* to improve insulin sensitivity.

### 3.6. *A. muciniphila* colonization inhibits fatty acid absorption to prevent obesity

We further examined the effects of orally administering *A. muciniphila* on fat accumulation in HFD-fed mice. The mice were gavaged with *A. muciniphila* thrice a week for 5 weeks (Figure 5F). The continuous administration of *A. muciniphila* markedly suppressed weight gain and improved glucose tolerance (Figure 5G and H). These effects were associated with decreased adipose tissue size and *Cd36* down-regulation in the jejunum (Figure 5I and J), indicating that *A. muciniphila* inhibited fatty acid absorption and prevented fat accumulation.

To determine the direct effects of *A. muciniphila* on energy and glucose metabolism, we colonized GF mice with either *A. muciniphila* or *B. thetaiotaomicron*, which reside in the mucus layer (Figure 6A). After 1 week of monocolonization on a normal diet, increased body and liver weights were observed among mice in the *B. thetaiotaomicron* group compared to those in GF mice, while *A. muciniphila* monocolonization had no effect on body or liver weights (Figure 6B and C). The OGTT revealed improved glucose tolerance in the *A. muciniphila* group compared to that in the *B. thetaiotaomicron* group (Figure 6D–E). *A. muciniphila* specifically suppressed the expression of *Cd36*, the main fatty acid transporter among the various nutrient transporters (Figure 6F and G). Finally, we performed plasma metabolomic analysis and found that *A. muciniphila* colonization lowered the plasma levels of various classes of fatty acids (Figure 6H). In summary, IX induced *A. muciniphila* proliferation, which enhanced intestinal barrier function and inhibited fatty acid absorption from the small intestine, leading to reduced obesity and improved insulin resistance (Figure 7).

## 4. DISCUSSION

Disruption of the gut microbiota significantly impacts energy metabolism. Turnbaugh et al. discovered that the gut microbiota in obesity more efficiently harvest dietary energy, further inducing obesity [2,3]. Thus, manipulating gut microbiota can potentially contribute to treating obesity. Various actions of microbial metabolites regulating energy metabolism have been elucidated. SCFAs and the activation of TGR5 regulate the energy balance towards anti-obesity [4]. However,

strategies to modulate the nutrient absorption capacity of the intestine, including the microbiota, are still unclear.

Polyphenols in hops, a beer ingredient, are beneficial to health [8]. A possible mechanism involves microbial metabolites, such as SCFAs, but IX administration does not alter fecal SCFA levels [26]. In this study, we performed plasma metabolomic analysis of IX-treated mice and found no significant difference in SCFA levels in the IX treated-mice compared to those in the control mice, suggesting that the metabolic improvement effect promoted by IX was independent of SCFAs. Here, IX treatment improved obesity and metabolic disorders through the inhibition of pancreatic lipase activity and intestinal bacteria-mediated action. The inhibition of pancreatic lipase reduces lipid absorption by attenuating the hydrolysis of dietary TGs. Orlistat, a lipase inhibitor, similarly inhibits lipid absorption and exerts its weight-loss effect; however, the adverse effects related to gastrointestinal symptoms such as diarrhea and steatorrhea limit its extensive use [27]. While administering 0.012% orlistat to an HFD increases the stool TG content by approximately 176% from 151 mg/g feces to 417 mg/g feces [28], IX administration increased it by 44% (Figure 3E). Thus, the lipid excretion-promoting effect of IX and the related gastrointestinal symptoms appeared to be milder than those of orlistat.

IX treatment significantly altered the microbial community structure and the favorable metabolic effects were canceled by antibiotic treatment, suggesting an involvement of the gut microbiota. Some polyphenols increase a relative abundance of *A. muciniphila* and are beneficial for metabolic health [9,29]. In the present study, IX selectively promoted the growth of *A. muciniphila* in an anaerobic chamber study, and significantly increasing the abundance of *A. muciniphila* in vivo.

*A. muciniphila* is a gram-negative anaerobic bacterium associated with ameliorating metabolic disorders in obese humans and rodents [22,30]. Provier et al. showed that administering live or pasteurized *A. muciniphila* reduces weight gain, insulin resistance, and dyslipidemia; they proposed the importance of TLR2 activation via the membrane protein components from *A. muciniphila* [30]. Furthermore, pasteurized *A. muciniphila* exhibits anti-obesity properties by increasing systemic energy expenditure, as assessed by metabolic cages and fecal energy excretion. Their study revealed downregulation of carbohydrate transporter-related genes, which is associated with enhanced epithelial turnover in the jejunum [31]. These results differed from the inhibition of lipid absorption by IX and *A. muciniphila* in our study, possibly because they administered perturbed *A. muciniphila* and we intended to explore the direct action of a single bacterial species via monocolonizing *A. muciniphila*. However, this is consistent with the fact that *A. muciniphila* exhibits anti-obesity effects by regulating intestinal nutrient absorption.

*A. muciniphila* also enhances barrier function [21]. Despite being a mucin-degrading bacterium, *A. muciniphila* administration increases mucus thickness [32] and goblet cell density [30]. This effect may be promoted by the enhanced turnover of epithelial cells [31] or the production of SCFAs, which are a major nutrient source for intestinal cells [33]. Deterioration of the intestinal environment due to an HFD and obesity reduces the intestinal barrier function and causes insulin resistance through metabolic endotoxemia [34,35]. Thus, IX-induced *A. muciniphila* proliferation restored the impairment of barrier function and improved insulin resistance, as confirmed by increased mucin and claudin-1 levels, and decreased LBP expression in the liver.

Furthermore, the *A. muciniphila* monocolonized mouse model and its metabolomic analysis revealed that *A. muciniphila* exhibits an anti-obesity effect by downregulating *Cd36* expression in the small intestine and inhibiting fatty acid absorption. This is a novel mechanism

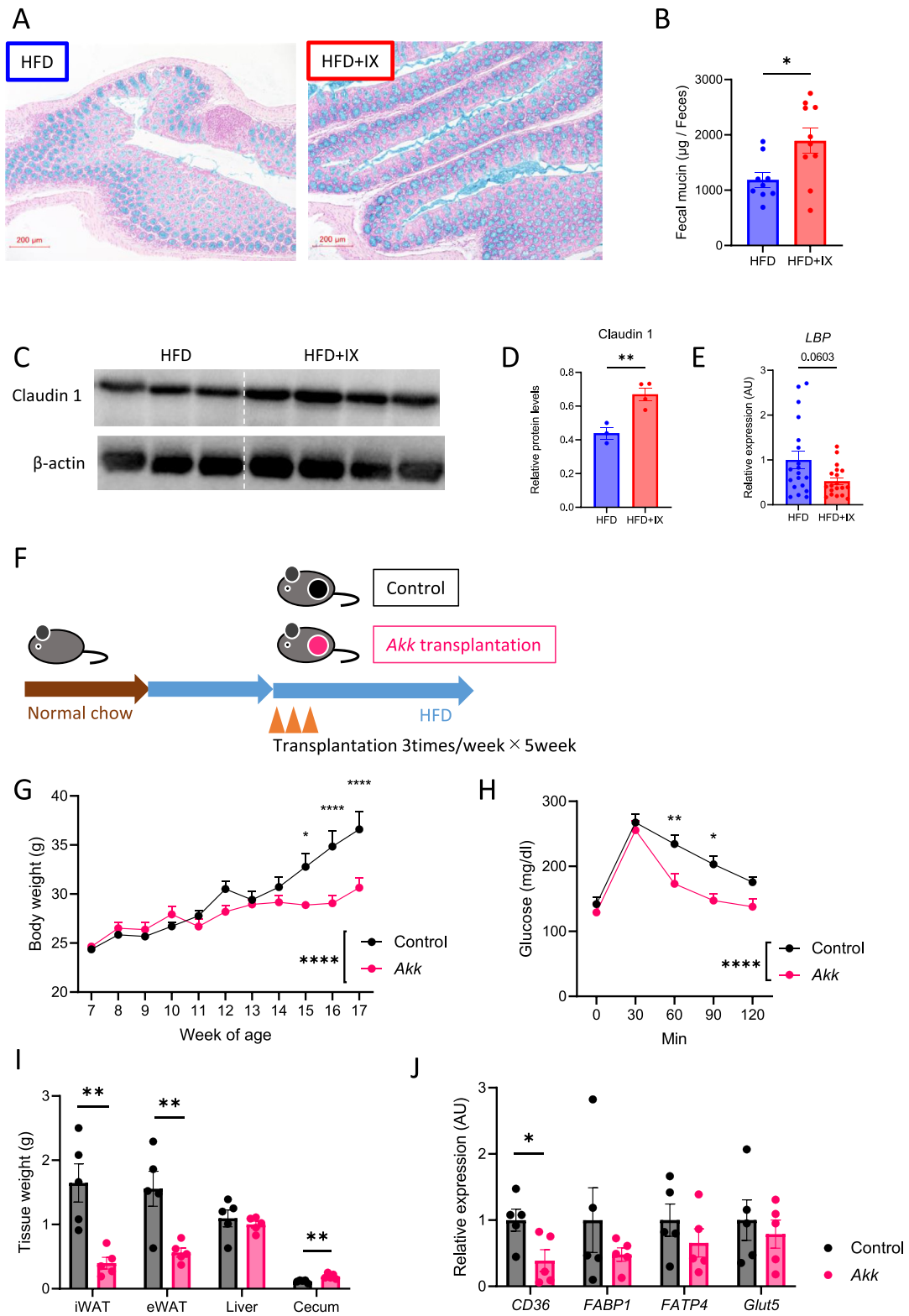


**Figure 5:** Compound IX enhances gut barrier function. (A) Representative alcian blue images of the colon. Scale bars, 200  $\mu$ m. (B) Fecal mucin levels per gram feces of mice fed either an HFD or an HFD + IX (n = 9–10 per group). (C) Western blots for claudin1 and  $\beta$ -actin in the colon of mice at 20 weeks old. (D) Quantitation of claudin1 normalized by  $\beta$ -actin. (E) qPCR of the lipopolysaccharide binding protein in the liver (n = 19 per group). (F) Schematic overview of the transplantation of specific pathogen-free mice with *A. muciniphila*. (G) Body weights of transplanted mice (n = 5 per group). (H) OGTT. (I) Tissue weight. (J) qPCR of various nutrient transporter-related genes in the jejunum of the transplanted mice (n = 5 per group). \*P < 0.05, \*\*P < 0.01, using two-way ANOVA, followed by Bonferroni's multiple comparison tests for (G, H) Wilcoxon rank sum test (E) or by unpaired two-tailed t-test for (B, D, I, J). Data are presented as the mean  $\pm$  SEM.

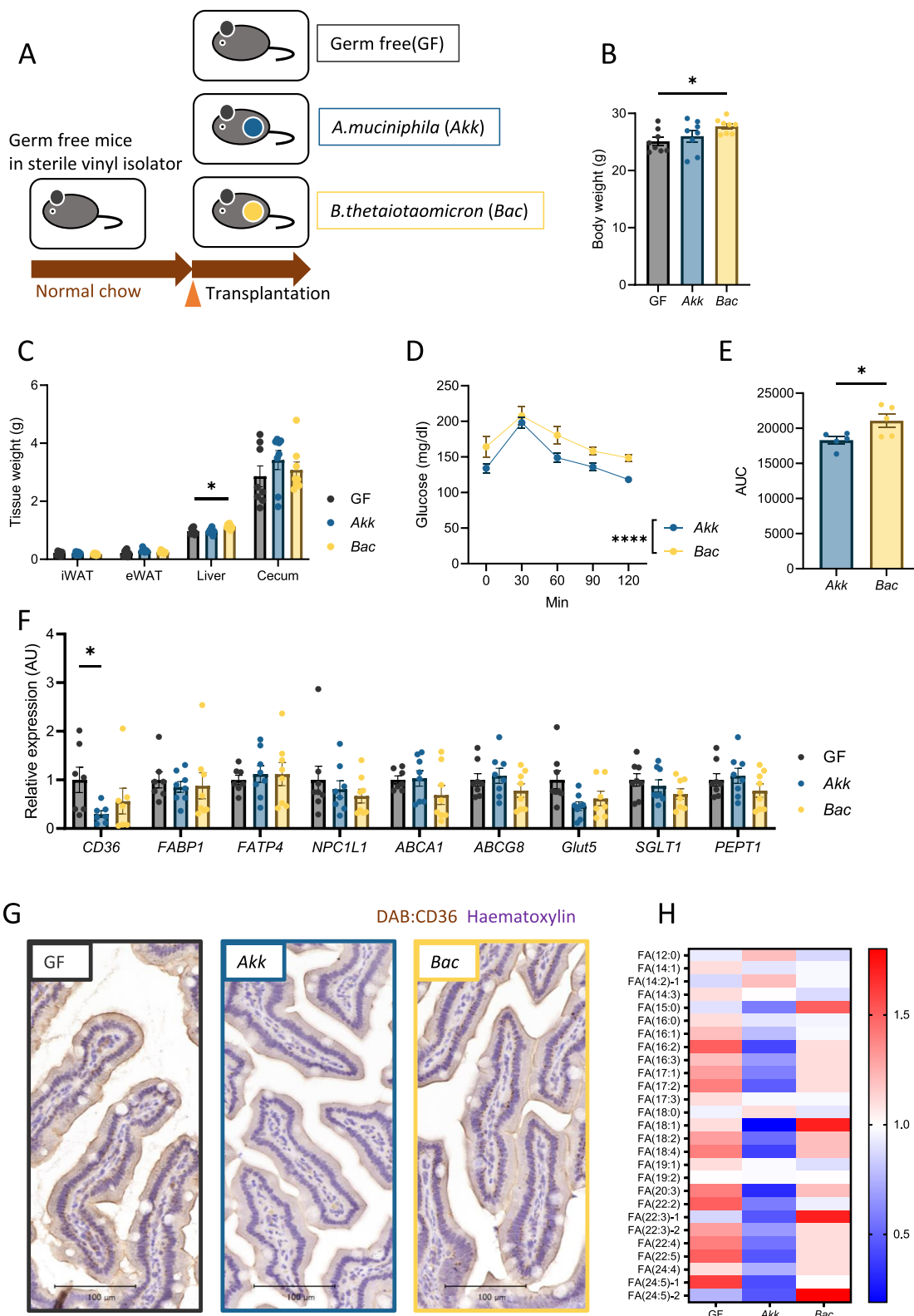


**Figure 6:** *A. muciniphila* suppresses fatty acid absorption via decreasing transporter-related genes in the small intestine. (A) Schematic overview of monocolonization of germ-free mice with *A. muciniphila* or *Bacteroides thetaiotaomicron*. (B) Body weight of monocolonized mice (n = 8 per group). (C) Tissue weight (D) OGTT (E) AUC of OGTT (F) qPCR of various nutrient transporter related genes in the jejunum of monocolonized mice (n = 8 per group). \*P < 0.05, \*\*P < 0.01, using two-way ANOVA, followed by Bonferroni's multiple comparison test for (C, D), or using ANOVA, followed by Tukey-Kramer post doc for (B, E, F). Data are presented as the mean ± SEM. (G) Representative CD36 images of the jejunum. Scale bars, 100 μm. (H) Heatmap showing saturated or unsaturated fatty acids detected in the plasma of monocolonized mice.

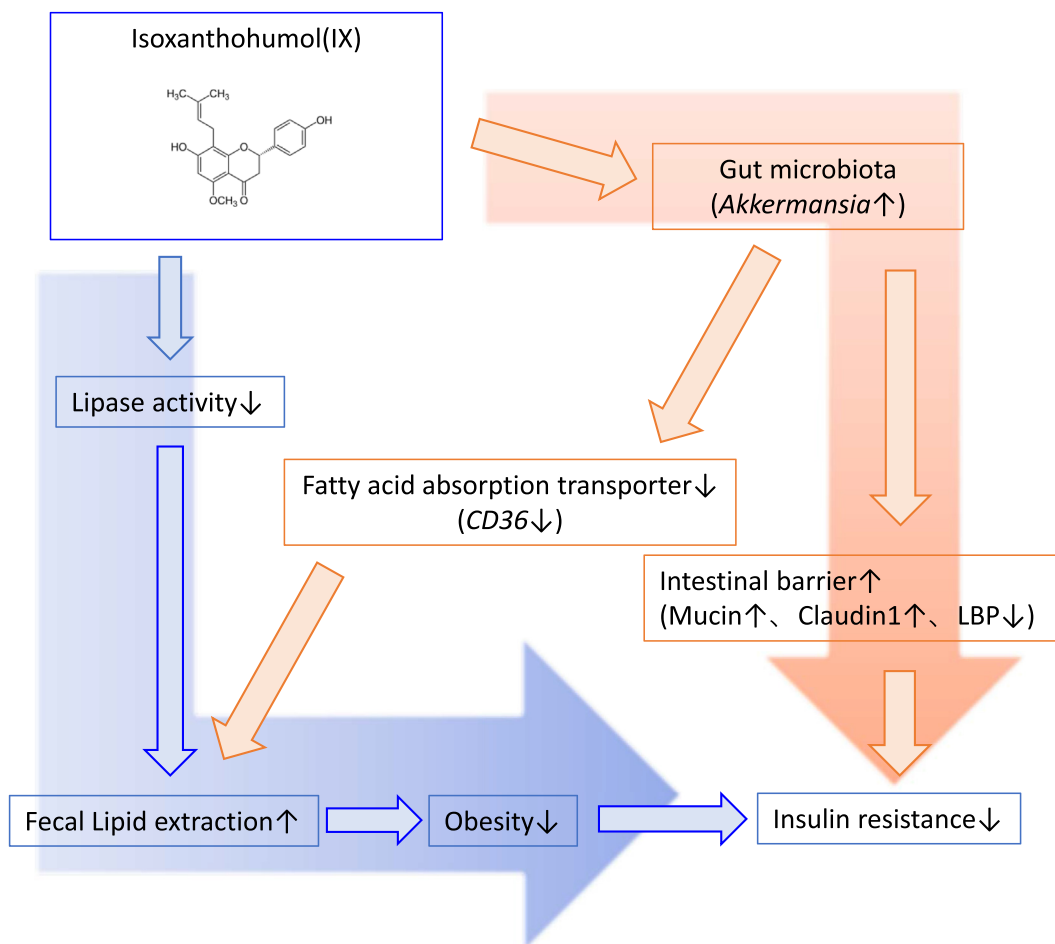


**Figure 7:** Proposed mechanisms of IX on obesity and insulin resistance. As a pharmacological pathway, IX inhibits lipase activity and reduces the expression of *Cd36* in the small intestine, thereby increasing fecal lipid excretion and obesity. In the microbial pathway, IX improves insulin resistance by altering the microbial composition, specifically increasing the abundance of *A. muciniphila* and enhancing intestinal barrier function. The anti-obesity effect of IX is further enhanced by the inhibition of fat absorption promoted by the proliferation of *A. muciniphila*.

underlying the effect of a single *A. muciniphila* strain on energy metabolism.

CD36 is a fatty acid transporter expressed in many cells and tissues, including platelets, macrophages, intestinal epithelial cells, endothelial cells, smooth muscle cells, adipose tissues, skeletal muscles, and cardiomyocytes. In the intestine, CD36 is highly expressed on the brush border membrane of enterocytes and is mainly localized in the duodenum and jejunum [36]. In addition, HFD significantly increases CD36 expression in the jejunum of mice [31,37], and its expression positively correlates with increasing BMI. In addition, it is significantly increased in vascular lesions and the kidneys of patients with hyperglycemia and/or hyperlipidemia, suggesting the dysregulation of CD36 levels in obesity and related metabolic dysfunction [38]. Although CD36 has intestinal hormone modulatory effects on GIP, GLP-1, and secretin, it is a major regulator of lipid absorption, as evidenced by a 50% reduction in lipid absorption in an intestinal *Cd36*-deficient mouse model [39]. C24:0 fatty acid absorption is completely inhibited from the intestine of *Cd36*-deficient mice fed an HFD, highlighting the important role of intestinal CD36 in absorbing dietary long-chain fatty acids [40]. Various signaling pathways regulate CD36 expression in enterocytes. Intestinal hormones such as secretin and cholecystokinin can act on their receptors to upregulate CD36 expression, promoting intestinal

lipid absorption [41,42]. In addition, diurnal variations in histone deacetylase 3, which is regulated by the microbiota, positively regulates CD36 via the activation of  $ERR\alpha$  [43]. Stojanović et al. reported that CD36 is downregulated in *Ppara*-deficient mice, suggesting that  $PPAR\alpha$  is a key regulator of intestinal CD36 [44]. In our study, IX treatment significantly decreased the expression of both *Ppara* and *Erra*, suggesting that IX regulates CD36 through these pathways.

As an interaction between intestinal bacteria and CD36 expression, FMT from HFD-fed mice into GF mice induces CD36 expression in the small intestine [45]. This suggests a close relationship between the adaptation of microbiota to nutrients and nutrient absorption. Kawano et al. reported that Th17-inducing microbiota, segmented filamentous bacteria (SFB) downregulates *Cd36* expression in the small intestine and prevents weight gain; however, *Faecalibaculum rodentium*, which is increased by a high-sugar diet, eliminates SFB and accelerates obesity [46]. Thus, intestinal bacterial interactions may be involved in CD36 regulation. To our knowledge, this is the first study to show that monocolonization of *A. muciniphila*, which was markedly increased by IX, decreases CD36 expression in the small intestine and plasma fatty acid concentrations using metabolomics analysis. Since HFD and obesity decrease the relative abundance of *A. muciniphila*, this may disrupt lipid absorption regulation, further contributing to obesity.

In conclusion, our study demonstrates that IX prevents obesity and enhances glucose metabolism by inhibiting dietary fat absorption. This mechanism is linked to suppressing pancreatic lipase activity and shifts in microbial composition, notably an increase in *A. muciniphila*. Moreover, the anti-obesity impact of IX is partially attributed to its ability to hinder fatty acid absorption, achieved by reducing the expression of the fatty acid transporter CD36 in the small intestine induced by *A. muciniphila* (Fig. 7). The modulation of the microbiota in response to dietary components plays a pivotal role in governing intestinal function and energy metabolism, proposing an innovative potential therapeutic strategy against obesity.

## 5. LIMITATIONS

Our study had certain limitations. Regarding the mechanism of the anti-obesity effect of IX, there was no change in thermogenesis-related gene expression in the inguinal adipose tissue; however, the basal metabolic rate was not evaluated using a metabolic cage. Therefore, an accurate evaluation of energy balance was not performed. We have shown that IX increased fecal mucin contents and claudin1, a tight junction-related protein in the colon; however, it did not evaluate actual gut permeability. Regarding the mechanism of *A. muciniphila* growth induced by IX treatment, IX-induced lipase activity inhibition may affect the growth of *A. muciniphila*. Previous studies on the effects of orlistat, a lipase inhibitor, on the gut microbiota have shown that it does not increase the abundance of *A. muciniphila* in mice and humans [47,48]. Another report showed that orlistat increases *A. muciniphila* levels in diet-induced obese mice [49]. To clarify the mechanism of enhanced *A. muciniphila* proliferation by IX treatment, we investigated the direct effects of IX on the growth of *A. muciniphila* and other bacterial species in an anaerobic chamber and showed that IX promoted the proliferation of *A. muciniphila*. These results do not rule out the possibility that the inhibition of lipase activity by IX affects *A. muciniphila* proliferation; however, they suggest that there is at least a direct effect of IX. However, the molecular mechanisms underlying the IX-induced *A. muciniphila* proliferation require further investigation. Finally, if the IX intake of the mice used in this experiment were applied to beer consumption in humans, it would be approximately 1000 L/day. We cannot expect IX to improve glucose metabolism by consuming beer, and its supplemental intake must be validated.

## AUTHOR CONTRIBUTIONS

Y.W. and S.F. designed and performed the experiments, analyzed the data, and wrote the manuscript. Y.M. helped bacterial experiments. S.W. performed the biochemical analyses. K.H. contributed technical assistance. H.H. performed histological experiments. A.N., To.K., Ay.N., M.B., A.R., Y.N., S.S., K.H., T.N., Y.N. and K.T. contributed to the discussion and interpretation of the data.

## FUNDING

This work was supported by grants from the Japan Society for the Promotion of Science (JSPS) KAKENHI grant numbers 17K09821 and 20K08882 to S.F., 21K20896 and 22K16424 to Y.W.; grants from AMED PRIME (JP18gm6010023h0001) to SF and grants from the Japan Diabetes Foundation, Takeda Science Foundation, and Mochida Memorial Foundation for Medical and Pharmaceutical Research (to SF), Lotte Foundation and Yakult Bio-Science Foundation (to YW). KT received lecture fees from MSD K.K., Novo Nordisk Pharma Ltd., and Kowa Pharmaceutical Co. Ltd., and grants from Daichi Sankyo Co.

Ltd., Ono Pharmaceutical Co. Ltd., Takeda Pharmaceutical Co. Ltd., Nippon Boehringer Ingelheim Co. Ltd., MSD K.K., Mitsubishi Tanabe Pharma Corporation, Teijin Pharma Limited, Eli Lilly Japan K.K., Asahi Kasei Pharma Corporation, and the Mitsubishi Foundation.

## DECLARATION OF COMPETING INTEREST

The authors declare that they have no known competing financial interests or personal relationships that could have appeared to influence the work reported in this paper.

## DATA AVAILABILITY

Data will be made available on request.

## ACKNOWLEDGMENTS

We thank Yurie Iwakuro and Kumi Sassa for their technical assistance.

## APPENDIX A. SUPPLEMENTARY DATA

Supplementary data to this article can be found online at <https://doi.org/10.1016/j.molmet.2023.101797>.

## REFERENCES

- [1] Koh A, Backhed F. From association to causality: the role of the gut microbiota and its functional products on host metabolism. *Mol Cell* 2020;78(4):584–96.
- [2] Ridaura VK, Faith JJ, Rey FE, Cheng J, Duncan AE, Kau AL, et al. Gut microbiota from twins discordant for obesity modulate metabolism in mice. *Science* 2013;341(6150):1241214.
- [3] Turnbaugh PJ, Ley RE, Mahowald MA, Magrini V, Mardis ER, Gordon JI. An obesity-associated gut microbiome with increased capacity for energy harvest. *Nature* 2006;444(7122):1027–31.
- [4] Fujisaka S, Watanabe Y, Tobe K. The gut microbiome: a core regulator of metabolism. *J Endocrinol* 2023;256(3).
- [5] Kimura I, Ichimura A, Ohue-Kitano R, Igarashi M. Free fatty acid receptors in health and disease. *Physiol Rev* 2020;100(1):171–210.
- [6] van Nierop FS, Scheltema MJ, Eggink HM, Pols TW, Sonne DP, Knop FK, et al. Clinical relevance of the bile acid receptor TGR5 in metabolism. *Lancet Diabetes Endocrinol* 2017;5(3):224–33.
- [7] de Vos WM, Tilg H, Van Hul M, Cani PD. Gut microbiome and health: mechanistic insights. *Gut* 2022;71(5):1020–32.
- [8] Rathod NB, Elabed N, Punia S, Ozogul F, Kim SK, Rocha JM. Recent developments in polyphenol applications on human health: a review with current knowledge. *Plants (Basel)* 2023;12(6).
- [9] Medina-Larque AS, Rodriguez-Daza MC, Roquim M, Dudonne S, Pilon G, Levy E, et al. Cranberry polyphenols and agave agavins impact gut immune response and microbiota composition while improving gut barrier function, inflammation, and glucose metabolism in mice fed an obesogenic diet. *Front Immunol* 2022;13:871080.
- [10] Barber TM, Kabisch S, Randeva HS, Pfeiffer AFH, Weickert MO. Implications of resveratrol in obesity and insulin resistance: a state-of-the-art review. *Nutrients* 2022;14(14).
- [11] Anhe FF, Roy D, Pilon G, Dudonne S, Matamoros S, Varin TV, et al. A polyphenol-rich cranberry extract protects from diet-induced obesity, insulin resistance and intestinal inflammation in association with increased Akkermansia spp. population in the gut microbiota of mice. *Gut* 2015;64(6):872–83.

- [12] Anhe FF, Nachbar RT, Varin TV, Vilela V, Dudonne S, Pilon G, et al. A polyphenol-rich cranberry extract reverses insulin resistance and hepatic steatosis independently of body weight loss. *Mol Metabol* 2017;6(12):1563–73.
- [13] Stevens JF, Taylor AW, Clawson JE, Deinzer ML. Fate of xanthohumol and related prenylflavonoids from hops to beer. *J Agric Food Chem* 1999;47(6):2421–8.
- [14] Miyata S, Inoue J, Shimizu M, Sato R. Xanthohumol improves diet-induced obesity and fatty liver by suppressing sterol regulatory element-binding protein (SREBP) activation. *J Biol Chem* 2015;290(33):20565–79.
- [15] Logan IE, Shulzhenko N, Sharpton TJ, Bobe G, Liu K, Nuss S, et al. Xanthohumol requires the intestinal microbiota to improve glucose metabolism in diet-induced obese mice. *Mol Nutr Food Res* 2021;65(21):e2100389.
- [16] Caballero I, Agut M, Armentia A, Blanco CA. Importance of tetrahydroiso alpha-acids to the microbiological stability of beer. *J AOAC Int* 2009;92(4):1160–4.
- [17] Fukizawa S, Yamashita M, Wakabayashi KI, Fujisaka S, Tobe K, Nonaka Y, et al. Anti-obesity effect of a hop-derived prenylflavonoid isoxanthohumol in a high-fat diet-induced obese mouse model. *Biosci Microbiota Food Health* 2020;39(3):175–82.
- [18] Yamashita M, Fukizawa S, Nonaka Y. Hop-derived prenylflavonoid isoxanthohumol suppresses insulin resistance by changing the intestinal microbiota and suppressing chronic inflammation in high fat diet-fed mice. *Eur Rev Med Pharmacol Sci* 2020;24(3):1537–47.
- [19] Derrien M, Vaughan EE, Plugge CM, de Vos WM. *Akkermansia muciniphila* gen. nov., sp. nov., a human intestinal mucin-degrading bacterium. *Int J Syst Evol Microbiol* 2004;54(Pt 5):1469–76.
- [20] Dao MC, Everard A, Aron-Wisniewsky J, Sokolovska N, Prifti E, Verger EO, et al. *Akkermansia muciniphila* and improved metabolic health during a dietary intervention in obesity: relationship with gut microbiome richness and ecology. *Gut* 2016;65(3):426–36.
- [21] Everard A, Belzer C, Geurts L, Ouwerkerk JP, Druart C, Bindels LB, et al. Cross-talk between *Akkermansia muciniphila* and intestinal epithelium controls diet-induced obesity. *Proc Natl Acad Sci U S A* 2013;110(22):9066–71.
- [22] Depommier C, Everard A, Druart C, Plovier H, Van Hul M, Vieira-Silva S, et al. Supplementation with *Akkermansia muciniphila* in overweight and obese human volunteers: a proof-of-concept exploratory study. *Nat Med* 2019;25(7):1096–103.
- [23] Watanabe S, Tsuneyama K. Cattle bile but not bear bile or pig bile induces lipid profile changes and fatty liver injury in mice: mediation by cholic acid. *J Toxicol Sci* 2012;37(1):105–21.
- [24] Possemiers S, Heyerick A, Robbens V, De Keukeleire D, Verstraete W. Activation of proestrogens from hops (*Humulus lupulus* L.) by intestinal microbiota; conversion of isoxanthohumol into 8-prenylnaringenin. *J Agric Food Chem* 2005;53(16):6281–8.
- [25] Fujisaka S, Avila-Pacheco J, Soto M, Kostic A, Dreyfuss JM, Pan H, et al. Diet, genetics, and the gut microbiome drive dynamic changes in plasma metabolites. *Cell Rep* 2018;22(11):3072–86.
- [26] Fukizawa S, Yamashita M, Fujisaka S, Tobe K, Nonaka Y, Murayama N. Isoxanthohumol, a hop-derived flavonoid, alters the metabolomics profile of mouse feces. *Biosci Microbiota Food Health* 2020;39(3):100–8.
- [27] Sjostrom L, Rissanen A, Andersen T, Boldrin M, Golay A, Koppeschaar HP, et al. Randomised placebo-controlled trial of orlistat for weight loss and prevention of weight regain in obese patients. European Multicentre Orlistat Study Group. *Lancet* 1998;352(9123):167–72.
- [28] Kazmi I, Afzal M, Rahman S, Iqbal M, Imam F, Anwar F. Antiobesity potential of ursolic acid stearyl glucoside by inhibiting pancreatic lipase. *Eur J Pharmacol* 2013;709(1–3):28–36.
- [29] Rodriguez-Daza MC, Pulido-Mateos EC, Lupien-Meilleur J, Guyonnet D, Desjardins Y, Roy D. Polyphenol-mediated gut microbiota modulation: toward prebiotics and further. *Front Nutr* 2021;8:689456.
- [30] Plovier H, Everard A, Druart C, Depommier C, Van Hul M, Geurts L, et al. A purified membrane protein from *Akkermansia muciniphila* or the pasteurized bacterium improves metabolism in obese and diabetic mice. *Nat Med* 2017;23(1):107–13.
- [31] Depommier C, Van Hul M, Everard A, Delzenne NM, De Vos WM, Cani PD. Pasteurized *Akkermansia muciniphila* increases whole-body energy expenditure and fecal energy excretion in diet-induced obese mice. *Gut Microb* 2020;11(5):1231–45.
- [32] van der Lugt B, van Beek AA, Aalvink S, Meijer B, Sovran B, Vermeij WP, et al. *Akkermansia muciniphila* ameliorates the age-related decline in colonic mucus thickness and attenuates immune activation in accelerated aging *Erc1 (-/Delta7)* mice. *Immun Ageing* 2019;16:6.
- [33] Liu MJ, Yang JY, Yan ZH, Hu S, Li JQ, Xu ZX, et al. Recent findings in *Akkermansia muciniphila*-regulated metabolism and its role in intestinal diseases. *Clin Nutr* 2022;41(10):2333–44.
- [34] Cani PD, Amar J, Iglesias MA, Poggi M, Knauf C, Bastelica D, et al. Metabolic endotoxemia initiates obesity and insulin resistance. *Diabetes* 2007;56(7):1761–72.
- [35] Pussinen PJ, Havulinna AS, Lehto M, Sundvall J, Salomaa V. Endotoxemia is associated with an increased risk of incident diabetes. *Diabetes Care* 2011;34(2):392–7.
- [36] Lobo MV, Huerta L, Ruiz-Velasco N, Teixeira E, de la Cueva P, Celdran A, et al. Localization of the lipid receptors CD36 and CLA-1/SR-BI in the human gastrointestinal tract: towards the identification of receptors mediating the intestinal absorption of dietary lipids. *J Histochem Cytochem* 2001;49(10):1253–60.
- [37] Lynes M, Narisawa S, Millan JL, Widmaier EP. Interactions between CD36 and global intestinal alkaline phosphatase in mouse small intestine and effects of high-fat diet. *Am J Physiol Regul Integr Comp Physiol* 2011;301(6):R1738–47.
- [38] Little TJ, Isaacs NJ, Young RL, Ott R, Nguyen NQ, Rayner CK, et al. Characterization of duodenal expression and localization of fatty acid-sensing receptors in humans: relationships with body mass index. *Am J Physiol Gastrointest Liver Physiol* 2014;307(10):G958–67.
- [39] Nassir F, Wilson B, Han X, Gross RW, Abumrad NA. CD36 is important for fatty acid and cholesterol uptake by the proximal but not distal intestine. *J Biol Chem* 2007;282(27):19493–501.
- [40] Drovser VA, Nguyen DV, Bastie CC, Darlington YF, Abumrad NA, Pessin JE, et al. CD36 mediates both cellular uptake of very long chain fatty acids and their intestinal absorption in mice. *J Biol Chem* 2008;283(19):13108–15.
- [41] Sekar R, Chow BK. Secretin receptor-knockout mice are resistant to high-fat diet-induced obesity and exhibit impaired intestinal lipid absorption. *Faseb J* 2014;28(8):3494–505.
- [42] Demenis C, McLaughlin J, Smith CP. Sulfated cholecystokinin-8 promotes CD36-mediated fatty acid uptake into primary mouse duodenal enterocytes. *Front Physiol* 2017;8:660.
- [43] Kuang Z, Wang Y, Li Y, Ye C, Ruhn KA, Behrendt CL, et al. The intestinal microbiota programs diurnal rhythms in host metabolism through histone deacetylase 3. *Science* 2019;365(6460):1428–34.
- [44] Stojanovic O, Altirriba J, Rigo D, Spiljar M, Evrard E, Roska B, et al. Dietary excess regulates absorption and surface of gut epithelium through intestinal PPARalpha. *Nat Commun* 2021;12(1):7031.
- [45] Watanabe Y, Fujisaka S, Ikeda K, Ishikawa M, Yamada T, Nawaz A, et al. Gut microbiota, determined by dietary nutrients, drive modification of the plasma lipid profile and insulin resistance. *iScience* 2021;24(5):102445.
- [46] Kawano Y, Edwards M, Huang Y, Bilate AM, Araujo LP, Tanoue T, et al. Microbiota imbalance induced by dietary sugar disrupts immune-mediated protection from metabolic syndrome. *Cell* 2022;185(19):3501–3519 e3520.

- [47] Ke J, An Y, Cao B, Lang J, Wu N, Zhao D. Orlistat-induced gut microbiota modification in obese mice. *Evid Based Complement Alternat Med* 2020;2020:9818349.
- [48] Jin J, Cheng R, Ren Y, Shen X, Wang J, Xue Y, et al. Distinctive gut microbiota in patients with overweight and obesity with dyslipidemia and its responses to long-term orlistat and ezetimibe intervention: a randomized controlled open-label trial. *Front Pharmacol* 2021;12:732541.
- [49] Jin J, Wang J, Cheng R, Ren Y, Miao Z, Luo Y, et al. Orlistat and ezetimibe could differently alleviate the high-fat diet-induced obesity phenotype by modulating the gut microbiota. *Front Microbiol* 2022;13:908327.